Structures and optical properties of tungsten oxide thin films deposited by magnetron sputtering of WO_3 bulk: Effects of annealing temperatures*

Zhang Feng(张 锋)[a)†], Wang Hai-Qian(王海千)[b)], Wang Song(王 松)[c)], Wang Jing-Yang(汪竟阳)[c)], Zhong Zhi-Cheng(钟志成)[c)], and Jin Ye(金 叶)[a)]

[a)] *School of Optoelectronic Information, Chongqing University of Technology, Chongqing* 400054, *China*
[b)] *Hefei National Laboratory for Physical Sciences at Microscale, University of Science and Technology of China, Hefei* 230026, *China*
[c)] *Hubei Key Laboratory of Low Dimensional Optoelectronic Material and Devices, Xiangyang* 441053, *China*

(Received 16 January 2014; revised manuscript received 31 March 2014; published online 23 July 2014)

Tungsten oxide thin films were deposited on glass substrates by the magnetron sputtering of WO_3 bulk at room temperature. The deposited films were annealed at different temperatures in air. The structural measurements indicate that the films annealed below 300 °C were amorphous, while the films annealed at 400 °C were mixed crystalline with hexagonal and triclinic phases of WO_3. It was observed that the crystallization of the annealed films becomes more and more distinct with an increase in the annealing temperature. At 400 °C, nanorod-like structures were observed on the film surface when the annealing time was increased from 60 min to 180 min. The presence of W=O stretching, W–O–W stretching, W–O–W bending and various lattice vibration modes were observed in Raman measurements. The optical absorption behaviors of the films in the range of 450–800 nm are very different with changing annealing temperatures from the room temperature to 400 °C. After annealing at 400 °C, the film becomes almost transparent. Increasing annealing time at 400 °C can lead to a small blue shift of the optical gap of the film.

Keywords: tungsten oxide film, magnetron sputtering, structure, optical property

PACS: 81.40.–z, 78.20.–e, 78.66.–w **DOI:** 10.1088/1674-1056/23/9/098105

1. Introduction

In the past few years, an increasing interest has been put on the tungsten oxide films due to their potential applications in smart windows,[1,2] gas sensors,[3,4] photocatalytic reactions,[5] and optoelectronic devices,[6] etc. The unique properties of the tungsten oxide films were usually determined by the oxygen defects and the valence states of tungsten ions.[7–9] Besides, it is very important to improve the properties of tungsten oxide films and other oxide films by controlling their morphologies and crystalline phases,[10,11] which mainly depend on the preparation technologies and thermal treating temperatures and atmospheres.[12,13]

Several preparation techniques have been used to deposit tungsten oxide thin films, including sol–gel,[14–16] hydrothermal technologies,[17] chemical vapor deposition,[18] thermal evaporation,[19] pulsed laser deposition,[20] and magnetron sputtering.[21,22] In fact, reactive magnetron sputtering is one of the most versatile techniques to deposit oxide films, allowing the control of many properties of the films by changing the partial pressure of the reactive gas, the components with the different targets and even sputtering power.[21–25] Many reports have been published explaining the mechanisms involved in thin film growth using magnetron sputtering, but very often these refer to tungsten oxide thin films obtained from a metallic tungsten target.[20–24] In contrast, the reports on tungsten oxide thin films obtained from a WO_3 target are seldom reported. In 2009, Acosta *et al.*[26] reported the studies on the optical properties of tungsten oxide thin films by non-reactive sputtering of WO_3 target and found that the argon pressure had a strong influence on the optical properties of the film. It has been predicted that a large amount of oxygen vacancies, defects and disordered structures in the deposited films, which are very critical in determining the crystalline, optical, photochemical and electric properties of tungsten oxide thin film, would be produced when the sputtering plasma interacts with WO_3 bulk.

The aim of this work is to investigate the effects of the annealing temperatures on the structure and optical property of tungsten oxide thin films that were deposited by magnetron sputtering of WO_3 bulk in a vacuum. As we all know, annealing, or thermal, treatment is one of the most effective ways to influence the structure and the properties of many films.[4,27–30] The deposited films were annealed at 200 °C and 300 °C for 60min and at 400 °C for 60 min and 180 min in air, respectively. We find that the annealing temperature of 400 °C can effectively influence the structure and optical property of the deposited films.

*Project supported by the Young Scientists Fund of the National Natural Science Foundation of China (Grant Nos. 11104365 and 11104366) and the Hubei Key Laboratory of Low Dimensional Optoelectronic Material and Devices, China (Grant No. 13XKL02002).

†Corresponding author. E-mail: zf080707@cqut.edu.cn

© 2014 Chinese Physical Society and IOP Publishing Ltd

2. Experiments

The investigated films were deposited on cleaned glass substrates by magnetron sputtering from a WO_3 target (99.95%, Goodwill Metal Technology Co. Ltd) in a programmed sputter system (made by Kurt J. Lesker Co.). The distance between the substrate and the target was kept at 150 mm. The base pressure of the deposition system was less than 5×10^{-6} Torr. The working Ar pressure of the deposition was kept at about 10 mTorr. The substrates holder was rolling with a speed of 10 r/min for getting uniform films during the sputtering. The RF power is 100 W and the deposition time is 60 min for all the films. The deposited films were annealed at 200 °C and 300 °C for 60 min and at 400 °C for 60 min and 180 min in air atmosphere, respectively.

The crystalline structures of the sample films were confirmed by X-Ray diffraction (XRD, XRD-6000, Shimadzu) with Cu $K\alpha$ at 40 kV and 20 mA and Raman spectroscopy (Raman, LabRamHR, JY) with a 514-nm excitation. The surface morphology was investigated by scanning electron microscopy (SEM, Sirion200, FEI) at 5 kV. The transmittance and reflectance of the samples in the UV–vis region were recorded by spectrophotometer (U-4100, Shimadzu).

3. Results and discussion

3.1. XRD and SEM characterizations

The films annealed at 200 °C and 300 °C display violet–red under the sunlight as well as the as-deposited ones. Nevertheless, the film annealed at 400 °C exhibits transparency and appeared to be blue colored. As shown in Fig. 1, the XRD data shows that the film annealed at 200 °C is amorphous, i.e. does not exhibit diffraction peaks (shown in Fig. 1(a)) while those annealed at 400 °C exhibit several sharp diffraction peaks, indicating the crystallization of this film happened. The peaks shown in Figs. 1(b) and 1(c) can be attributed to a mixture of polycrystalline phases, which includes hexagonal h-WO_3 phase (JCPDS PDF-33-1387) and triclinic t-WO_3 phase (JCPDS PDF-30-1387). It is also seen that the films annealed at 400 °C were dominated by hexagonal h-WO_3 phases. Acosta *et al.* had prepared the tungsten oxide thin films by sputtering WO_3 bulk. Their results indicated that the films mainly contained hexagonal h-WO_3 phase and monoclinic α-WO_3 phase.[26] Usually, the polycrystalline monoclinic and triclinic phases can be observed in the films deposited by reactive magnetron sputtering from W target, but few reports have also shown the presence of hexagonal phases.[23,31–33] Comparing Fig. 1(b) with Fig. 1(c), we can see that the growths of the film along (002) and (200) orientations of the triclinic phases are enhanced when thermal treatment time at 400 °C is prolonged from 60 min to 180 min.

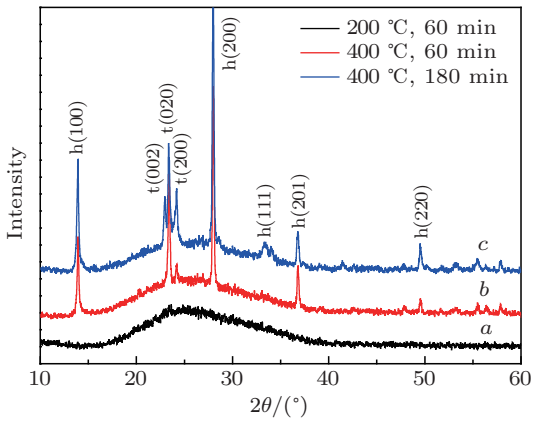


Fig. 1. (color online) XRD patterns of the tungsten oxide films annealed at 200 °C for 60 h (a) and 400 °C for 60 min (b) and 180 min (c), respectively.

Under our experimental conditions, the thickness d of the as-deposited film has been determined to be about 220 nm by an observation of its section SEM. Figure 2 displays the surface SEM images of the thin films annealed at different temperatures. All the sample films are very compact. The sizes of the sputtered tungsten oxide grains look very uniform and are a little less than 100 nm. The grain boundaries become more and more discernable as the annealing temperature increases from room temperature to 400 °C (see Figs. 2(a)–2(c)), whereas they become very indistinct again owing to the growth of the grains when the annealing time is prolonged from 60 min to 180 min at 400 °C. This process indicates the structure transformation of the sample films from the complete amorphous nature to crystallization and is in complete agreement with the results confirmed by XRD (Fig. 1). The surfaces of the deposited films become rougher as the annealing temperatures rise. When the annealing time at 400 °C increases from 60 min to 180 min, the nanorod-like structures have grown from the surface of the deposited film (Fig. 2(d)). This kind of surface morphology of the samples is very different from those of the films prepared by sol–gel methods[14–16] and by reactively sputtering tungsten metal target.[21,22,31–33]

It is well known that during the sputtering, the interaction between Ar plasma and WO_3 bulk can highly distort and tilt the form works of the WO_6 octahedra and thus results in an amorphous film. At the same time, a large number of oxygen vacancies and defects, which can reduce the tungsten ions from W^{6+} to W^{5+} or W^{4+},[34] would be produced in the deposited films. This is responsible for the violet–red color and the amorphous XRD data of the films annealed below 300 °C. The obvious crystallinity of the deposited films at 400 °C for 60 min implies that the defects and disordered structures in the films have been effectively activated by this temperature. Consequently, increasing the annealing time at 400 °C is obviously favorable to the crystallinity and the growth of the films.

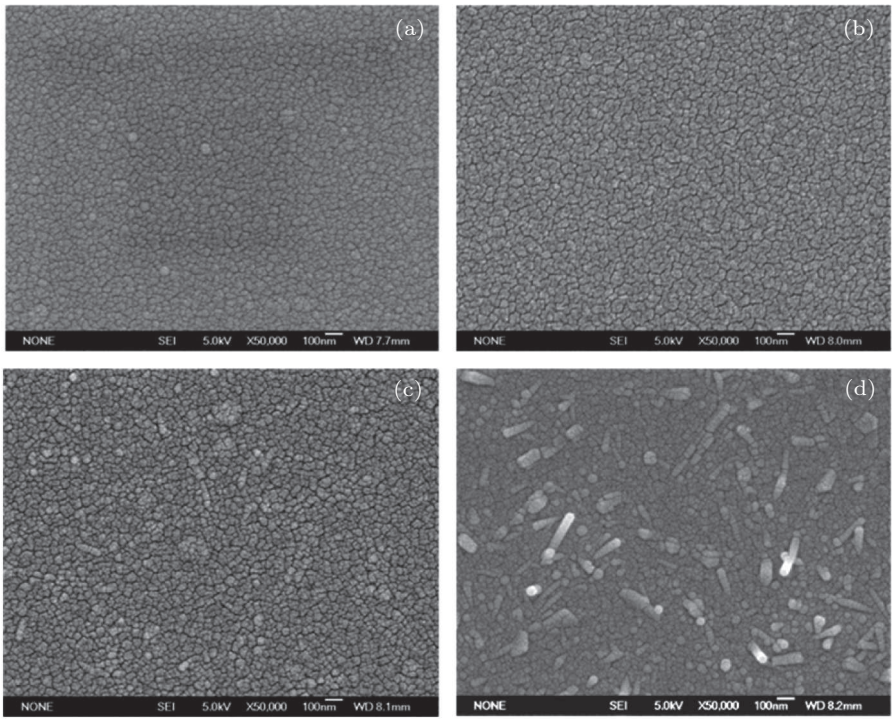


Fig. 2. SEM graphs of the as-deposited film (a) and the ones annealed at 300 °C for 60 min (b), 400 °C for 60 min (c), and 400 °C for 180 min (d).

3.2. Surface Raman spectra

Figure 3 shows surface Raman spectra of the sample films that were annealed at different temperatures. Except for a Raman peak at 280 cm^{-1}, the Raman spectra of the films annealed below 300 °C exhibit two broad bands in two regions of 100–500 cm^{-1} and 600–1000 cm^{-1}. Several weak Raman peaks gradually arise in the range of 600–1000 cm^{-1} with the increase of annealing temperatures. When the film was annealed at 400 °C for 60 min, several obvious Raman peaks at 116, 185, 280, 762, 849, 879, 951, and 1095 cm^{-1} appeared in the spectrum, as shown in Fig. 3(d). Among them the peaks at 116, 280, 762, and 951 cm^{-1} are stronger relative to the others. Increasing annealing time from 60 min to 180 min at 400 °C, several new Raman peaks appeared at 134, 330, 705, and 810 cm^{-1}, respectively, and meanwhile a weak Raman peak at 849 cm^{-1} disappeared (shown in Fig. 3(e)).

As mentioned above, a large variety of bond lengths and disordered structures should be responsible for the broad Raman bands of the films that were annealed below 300 °C (shown as Figs. 3(a)–3(c)). Meanwhile, it was thought that a large number of oxygen vacancies also play an important role in broadening the Raman peaks.[34] When the annealing temperature increased from 300 °C to 400 °C, the crystallization and oxidation of the deposited films were obviously improved and therefore resulted in several distinct peaks in the Raman spectrum due to the formation of the stable W–O bonds. Usually, Raman spectra of crystalline WO_3 films have several typical peaks around 950, 808, 719, and 275 cm^{-1}, corresponding to W=O bond stretching, W–O–W bond symmetry stretching, asymmetry stretching, and bending vibration modes[11,13,14,34–38] respectively. The peaks below 200 cm^{-1} are assigned as lattice vibration modes.[12–14,38] Nevertheless, shifts of Raman peaks often happen because of the differences in sizes, morphologies and crystal phases of WO_3 films.[34–38]

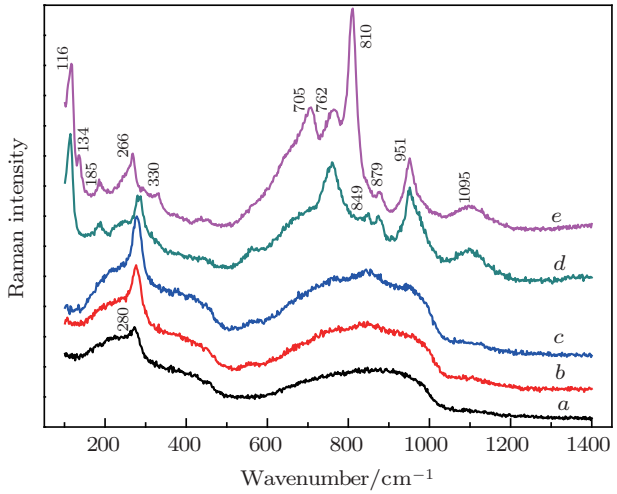


Fig. 3. (color online) Raman spectra of the as-deposited film (curve *a*) and the ones annealed at 200 °C for 60 min (curve *b*), 300 °C for 60 min (curve *c*), 400 °C for 60 min (curve *d*), 400 °C for 180 min (curve *e*).

In our experiments, for the film annealed at 400 °C for 60 min, Raman peaks at 951, 762, and 280 cm^{-1} correspond to W^{6+}=O stretching vibration, W^{6+}–O–W^{6+} stretching vibra-

tion and bending vibration,[13–17,34] respectively. The peaks at 116 cm^{-1} and 185 cm^{-1} involve the vibration modes of different lattices from the different phases. The peak at 849 cm^{-1} is assigned to short W–O–W stretching vibration, while peak at 879 cm^{-1} is assigned to W–O–W deformation vibration. After a longer thermal treatment at 400 °C, the structures of the film tend to be more stable and most of the W–O–W bonds could become shorter, which would lead to a result that the Raman peak at 762 cm^{-1} is depressed and the peak at 810 cm^{-1} corresponding to the symmetry stretching vibration of the W–O–W bonds is greatly enhanced. The peak at 705 cm^{-1} can be related to the asymmetric stretching vibration of the W–O–W bonds. The Raman peaks at 266 cm^{-1} and 330 cm^{-1} can be attributed to bending vibration modes of the W–O–W and the deformed W–O–W bonds, respectively. The broad peak observed at 1092 cm^{-1} is not characteristic of WO_3 and is thought to originate from the surface absorbtate.[14]

3.3. Optical behaviors

Figure 4 shows the wavelength dependence of transmittance (T) and reflectance (R) of the unannealed films and the ones annealed at 200 °C, 300 °C, and 400 °C, respectively. The oscillations in the T and R spectra are from the optical interference due to the refractive index difference between the film and substrate. As shown in Fig. 4(a), the as-deposited films have the lowest transmittance values relative to the annealed ones. When the annealing temperature increases from 200 °C to 300 °C, no substantial changes for the transmittance of the sample film happen in the range of 300–800 nm, especially in the range of < 520 nm. The transmittance of the thin film is greatly improved when the annealing temperatures increase from 300 °C to 400 °C. It is also seen that annealing time at 400 °C does not obviously enhance the transmittance values of the sample (see Fig. 4(a)). The reflectance behaviors of the thin films (shown in Fig. 4(b)) show similar tendencies to the transmission behavior as the annealing temperatures increasing. The oscillating amplitudes of the transmittance and reflectance spectra of the samples become more and more striking (shown in Fig. 4(b)), suggesting that the thickness of the annealed films increases with the annealing temperatures rising from 300 °C to 400 °C.

The absorption spectra of the samples shown in Fig. 5 was calculated from transmittance, and reflectance measurements according to the correlation of $A\%+T\%+R\% = 100\%$, where $A\%$, $T\%$, $R\%$ are absorbance, transmittance, and reflectance values at the corresponding wavelength, respectively. To compare with each other conveniently, the calculated absorbance values of the thin films were normalized. It can be seen from Fig. 5 that the optical absorbance behaviors of the films annealed at below 300 °C display obvious difference in the wavelength range of 450–800 nm. The as-deposited film has a weak absorption band only in the range of 450–650 nm. With the increase of the annealing temperatures up to 300 °C, the annealed samples have an increasing optical absorption in 450–800 nm, however, the samples annealed at 400 °C almost have no optical absorption in the same wavelength range and become almost transparent.

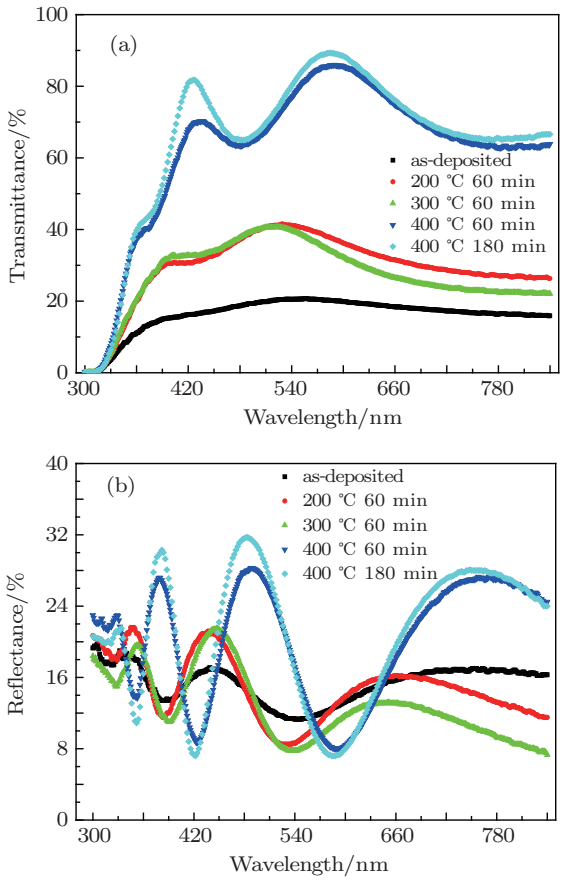


Fig. 4. (color online) UV–vis transmittance (a) and reflectance (b) spectra of the as-deposited film and the ones annealed at the different temperatures.

The as-deposited tungsten oxide films in our experiment have similar optical transmittance to those prepared by sputtering WO_3 target at low argon pressures ($\leq$ 20 mTorr).[26] The reasons for low optical transmittance of the unannealed films can be attributed to the fact that oxygen atoms (ten times lighter than tungsten) are scattered more effectively than tungsten atoms during the sputtering, leading to a large amount of oxygen vacancies in the deposited films.[26] Usually, annealing in air is helpful to improve the crystallinity of the films and favors their oxidation because the defects and disordered lattices in the films are activated and recombined. Contrast transformation of the optical absorption of the sample films should be due to the substantial reduction of low-valence W

ions and defects after annealing at 400 °C.[13,26]

The optical band gaps (E_g) of all samples are simply evaluated from their UV absorption edges by extrapolating the linear region of the plot $(\alpha h\nu)^{1/2}$ versus $h\nu$ to zero absorption,[20] where $\alpha = \ln((1-R)/T)/d$ is absorption coefficient and $h\nu$ is photon energy. We find the E_g values of the samples vary with the annealing temperatures. It can be seen from the inset in Fig. 5 that the unannealed film has the lowest E_g value of about 2.82 eV. After annealing at 200 °C and 300 °C, the E_g values become about 3.10 eV and 3.12 eV, respectively. When the films were annealed at 400 °C for 60 min and 180 min, the corresponding E_g values of the samples are 3.20 eV and 3.27 eV, respectively. These E_g values are almost in agreement with the ones (2.15–3.22 eV) reported for the other tungsten trioxide thin films.[19–24,26,39] The results from theoretical calculations indicate that the hexagonal WO_3 phase possesses the lowest optical bandgap value (1.75 eV) relative to the other phases.[7] For hexagonal WO_3 phases, the optical E_g values of the hierarchical nanostructures (2.55 eV)[39] are lower than those of crystal nanowire or nanorod structures (3.30 eV).[6] Thus, it is thought that a light increase in E_g value with the annealing time at 400 °C should originate from the enhancement of the triclinic phases and the crystallinity of the tungsten oxide film.

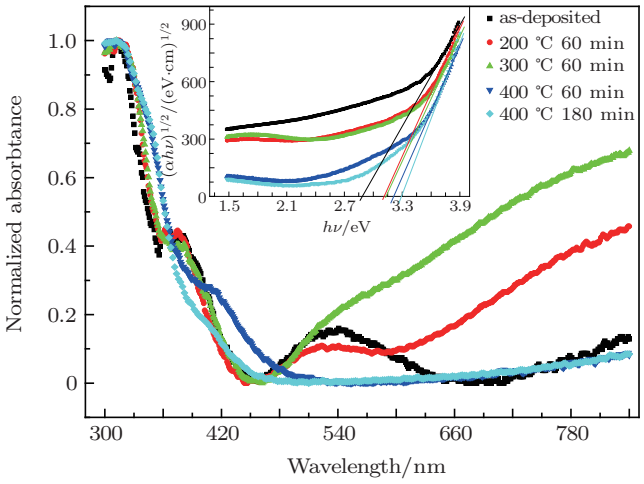


Fig. 5. (color online) UV–vis absorption curves of the as-deposited film and the ones annealed at the different temperatures. The inset is plots of the $(\alpha h\nu)^{1/2}$ versus photon energy ($h\nu$) for the corresponding sample films.

4. Conclusion

We have investigated the effects of annealing temperatures on the structure and optical property of tungsten oxide thin films by sputtering WO_3 target. It is found that the annealing treatments at 400 °C in the air caused as-deposited amorphous WO_3 thin films to crystallize into the hexagonal WO_3 phases accompanied by the triclinic phase. Increasing annealing time at 400 °C can improve the crystallinity of WO_3 thin films and lead to a rougher surface morphology, where nanorod-like structure can be clearly observed. The results from Raman spectra further confirmed the crystallinity of WO_3 thin films with distinct vibration peaks of the W–O bonds and lattices after annealing at 400 °C. When the annealing temperature increases from the room temperature to 400 °C the optical behaviors of the tungsten oxide thin film can be effectively influenced and the corresponding band gap varies from 2.82 eV to 3.27 eV.

Acknowledgment

We are greatly indebted to Dr. Mandar M. Shirolkar (Hefei National Laboratory for Physical Sciences at Microscale, USTC) for his kind technical support and helpful discussion.

References

[1] Deb S K 2008 *Sol. Energy Mater. Sol. Cells* **92** 245
[2] Rao M C 2013 *J. Non-oxide Glas.* **5** 1
[3] Kukkola J, Mäklina J, Halonena N, Kyllönena T, Tóth G Szabó M, Shchukarev A, Mikkola J P, Jantunen H and Kordás K 2011 *Sensor Actuat B-Chem.* **153** 293
[4] Hu M, Jia D L, Liu Q L, Li M D and Sun P 2013 *Chin. Phys. B* **22** 068204.
[5] Liu X, Wang F and Wang Q 2012 *Phys. Chem. Chem. Phys.* **14** 7894
[6] Huang K, Zhang Q, Yang F and He D 2010 *Nano Res.* **3** 281
[7] Migas D B, Shaposhnikov V L, Rodin V N and Borisenko V E 2010 *J. Appl. Phys.* **108** 093713
[8] He X, Yin Y, Guo J, Yuan H, Peng Y, Zhou Y, Zhao D, Hai K, Zhou W and Tang D 2013 *Nanoscale Res. Lett.* **8** 50
[9] He T and Yao J 2007 *J. Mater. Chem.* **17** 4547
[10] Vemuri R S, Bharathi K K, Gullapalli S K and Ramana C V 2010 *Appl. Mater. Inter.* **2** 2623
[11] Biswas S K and Baeg J O 2013 *Int. J. Hydrogen Energy* **38** 3177
[12] Frey G L, Rothschild A, Sloan J, Rosentsveig R, Popovitz-Biro R and Tenne R 2001 *J. Solid State Chem.* **162** 300
[13] Szilagyi I M, Santala E and Heikkila M 2011 *J. Therm. Anal. Calorim.* **105** 73
[14] Breedon M, Spizzirri P, Taylor M, Plessis J, McCulloch D, Zhu J, Yu L, Hu Z, Rix C, Wlodarski W and Kalantar-Zadeh K 2010 *Cryst. Growth Des.* **10** 430
[15] Kim C Y, Lee M, Huh S H and Kim E K 2010 *J. Sol–Gel Sci. Technol.* **53** 176
[16] Yang B, Barnes P R F, Zhang Y and Luca V 2007 *Catal. Lett.* **118** 280
[17] Zheng F, Zhang M and Guo M 2013 *Thin Solid Films* **534** 45
[18] Blackman C S and Parkin I P 2005 *Chem. Mater.* **17** 1583
[19] Kim H, Senthil K and Yong K 2010 *Mater. Chem. Phys.* **120** 452
[20] Zou Y S, Zhang Y C, Lou D, Wang H P, Gu L, Dong Y H, Dou K, Song X F and Zeng H B 2014 *J. Alloy. Compd.* **583** 465
[21] Chena H C, Jan D J, Chena C H and Huang K T 2013 *Electrochim. Acta* **93** 307
[22] Charles C, Martin N, Devel M, Ollitrault J and Billard A 2013 *Thin Solid Films* **534** 275
[23] Imai M, Kikuchi M, Oka N and Shigesato Y 2012 *J. Vac. Sci. Technol. A* **30** 031503
[24] Choi H W, Kim E J and Hahn S H 2010 *Chem. Eng. J.* **161** 285
[25] Lü M S, Pang Z Y, Xiu X W, Dai Y and Han S H 2007 *Chin. Phys.* **16** 548
[26] Acosta M, González D and Riech I 2009 *Thin Solid Films* **517** 5442
[27] Yan J L, Zhao Y N and Li C 2014 *Chin. Phys. B* **23** 048105

[28] Boonyopakorn N, Sripongpun N, Thanachayanont C and Dangtip S 2010 *Chin. Phys. Lett.* **27** 108103

[29] Chen Y Y, Wang X, Cai X K, Yuan Z J, Zhu X M, Qiu D J and Wu H Z 2014 *Chin. Phys. B* **23** 026101

[30] Peng L P, Fang L, Wu W D, Wang X M and Li L 2012 *Chin. Phys. B* **21** 047305

[31] Horprathum M, Limwichean K, Wisitsoraat A, Eiamchai P, Aiempanakit K, Limnonthakul P, Nuntawong N, Pattantsetakul V, Tuantranont and Chindaudom A P 2013 *Sensor Actuat. B-Chem.* **176** 685

[32] Johansson M B, Niklasson G and Oŝterlund L 2012 *J. Mater. Res.* **27** 3130

[33] Vidyarthi V S, Hofmann M, Savan A, Sliozberg K, Konig D, Beranek R, Schuhmann W and Ludwig A 2011 *Int. J. Hydrogen Energ.* **36** 4724

[34] Ramana C V, Utsunomiya S, Ewing R C, Julien C M and Becker U 2006 *J. Phys. Chem. B* **110** 10430

[35] Pyper O, Kaschner A and Thomsen C 2002 *Sol. Energy Mater. Sol. Cells* **71** 511

[36] Szilagyi I M, Wang L, Gouma P R, Balazsi C, Madarasz J and Pokol G 2009 *Mater. Res. Bull.* **44** 505

[37] György E, Socol G and Mihailescu I N 2005 *J. Appl. Phys.* **97** 093527

[38] Subrahmanyam A and Karuppasamy A 2007 *Sol. Energy Mater. Sol. Cells* **91** 266

[39] Shen Y, Ding D, Yang Y, Li Zhen and Zhao L 2013 *Mater. Res. Bull.* **48** 2317